

## Vanadia-based equilibrium-thickness amorphous films on anatase (101) surfaces

Haijun Qian and Jian Luo<sup>a)</sup>

School of Materials Science and Engineering, Clemson University, Clemson, South Carolina 29634

(Received 6 June 2007; accepted 12 July 2007; published online 7 August 2007)

Nanometer-thick, surficial amorphous films are found to form in a model “monolayer” catalyst system: vanadia on TiO<sub>2</sub> anatase (101) surfaces. These films exhibit a self-selecting or “equilibrium” thickness; once a thermodynamic equilibrium is reached, the film thickness, which corresponds to the Gibbsian surface excess of vanadia adsorbates, is independent of synthesis methods, the fraction of secondary vanadia phase, and the heat treatment history. These (multilayer) adsorbate films are largely amorphous (quasiliquid) at subeutectic temperatures, where analogies to premelting and prewetting phenomena are made. Reversible film thickness versus temperature (with a hysteresis loop) is observed and explained from a force-balance model. © 2007 American Institute of Physics. [DOI: 10.1063/1.2768315]

Impurity-based, equilibrium-thickness, intergranular glassy films (IGFs) have been observed at grain boundaries in ceramics<sup>1,2</sup> and metals,<sup>2,3</sup> and at metal–oxide interfaces.<sup>4</sup> Recently, analogous surficial amorphous films (SAFs) have been found for Bi<sub>2</sub>O<sub>3</sub> on ZnO and few other oxides.<sup>2,5–7</sup> Like IGFs, SAFs exhibit an “equilibrium” thickness on the order of 1 nm, which is attributed to a balance among several attractive and repulsive interfacial forces.<sup>2,5–7</sup> Alternatively, these SAFs can be understood to be multilayer adsorbates in a prewetting regime.<sup>2,6,7</sup>

On the other hand, thermal spreading of V<sub>2</sub>O<sub>5</sub>, MoO<sub>3</sub>, and other catalytic oxides onto the surfaces of refractory oxide supports (e.g., Al<sub>2</sub>O<sub>3</sub> or TiO<sub>2</sub>) is widely used to disperse metal oxide catalysts,<sup>8–12</sup> and the supports can modify reactivity.<sup>13</sup> It was generally believed that monolayer surface adsorption of the catalytic oxides occurs during the spreading.<sup>9,10</sup> Hence, these supported oxide catalysts are often termed as “monolayer” catalysts.

Titania-supported vanadia (VO<sub>x</sub>/TiO<sub>2</sub>) is widely used for partial oxidation and ammoxidation of alkylaromatic compounds, and it is often regarded as a model monolayer catalyst.<sup>8–12</sup> However, formation of nanometer-thick amorphous vanadia films on the surfaces of anatase and rutile was reported.<sup>11,12,14</sup> It is unknown whether the thickness of these films is supply controlled or these films are in fact equilibrium-thickness SAFs. This study explores the existence and stability of equilibrium-thickness SAFs in this model monolayer catalyst.

TiO<sub>2</sub> anatase nanosized powders<sup>15</sup> were purchased and annealed at 250 °C for 4 h to remove moisture. V<sub>2</sub>O<sub>5</sub> (99.99%) and NH<sub>4</sub>VO<sub>3</sub> (99.995%) were purchased from Alfa Aesar. To identify the effect of synthesis routes, specimens were prepared by two methods. In a wet impregnation method,<sup>12</sup> the support powder was impregnated with a mixed solution of NH<sub>4</sub>VO<sub>3</sub> and NH<sub>4</sub>OH, and the mixtures were dried at 85 °C for 24 h, heated at 220 °C for 3 h, and calcined at 450 °C for 3 h. In a dry impregnation method, a physical mixture of pure crystalline V<sub>2</sub>O<sub>5</sub> and nanosized anatase powder was used. In both routes, the mixtures were

isothermally annealed at desired equilibration temperatures in double closed containers and then air quenched. Extra pure V<sub>2</sub>O<sub>5</sub> powder was placed between the two containers to reduce evaporation loss (0.5%–1.5% weight loss was typically measured). Particle surfaces were characterized by high-resolution transmission electron microscopy (HRTEM) using a Hitachi 9500 microscope (300 kV, 0.10 nm lattice resolution). Minimum exposure was used during HRTEM to avoid electron beam damage.

Analogous SAFs have been found to form on faceted surfaces of several orientations and curved surfaces of anatase particles. X-ray diffraction analysis showed that <20 wt % of the anatase phase transferred into rutile for specimens annealed at 600 °C and no phase transformation occurred at lower temperatures. To separate the effects of titania phase and orientation, this study selected only those SAFs that formed on anatase (101) surfaces [with parallel lattice fringes matching the anatase (101) spacing of 0.35 nm] for a systematical investigation (Fig. 1).

Once an equilibrium state is reached at a given temperature (e.g., 600 °C), these SAFs exhibit a constant (self-selecting) thickness. First, film thickness is uniform along the surface (Fig. 1) and varies little from one surface to an-

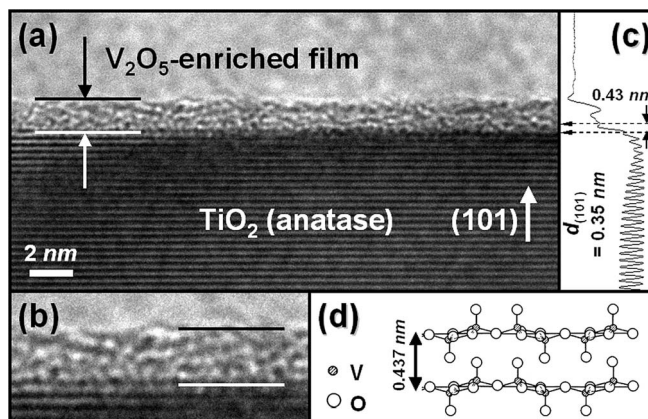


FIG. 1. (a) HRTEM image of a vanadia-based SAF formed at 600 °C. (b) An expanded view of a selected segment of this SAF. (c) Pixel (gray level) intensities averaged along the horizontal axis. The partial layering order in the film matches that of the V<sub>2</sub>O<sub>5</sub> crystal as shown in (d).

<sup>a)</sup> Author to whom correspondence should be addressed; electronic mail: jianluo@clemson.edu and jluo@alum.mit.edu

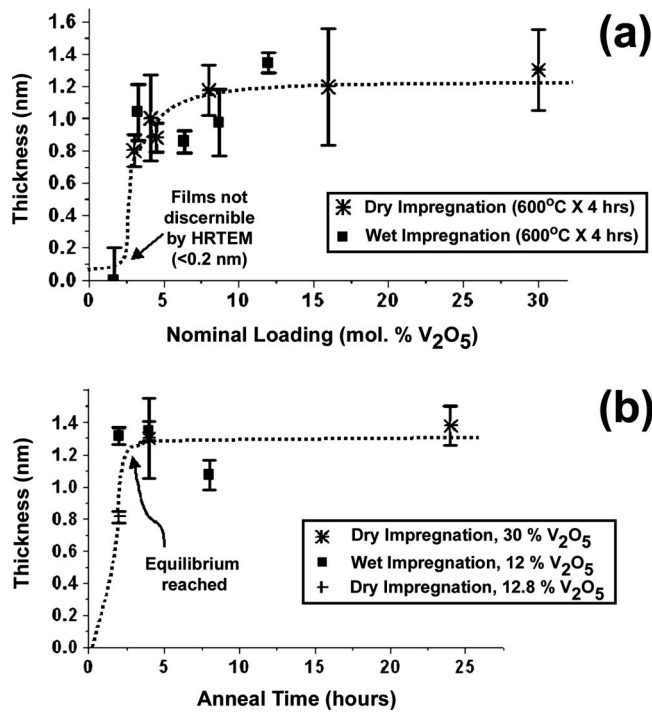


FIG. 2. Film thickness vs (a) nominal  $V_2O_5$  loading and (b) anneal time for specimens annealed at  $600^\circ\text{C}$ . Once an equilibrium state is reached, these films exhibit an equilibrium thickness, independent of the additional annealing time, the  $V_2O_5$  loading, and synthesis methods.

other. The average thickness for 119 SAFs that formed at  $600^\circ\text{C}$  with different processing recipes is  $1.10\text{ nm}$  with a rather narrow standard deviation of  $0.26\text{ nm}$ . Second, Fig. 2(a) shows the average film thickness versus nominal  $V_2O_5$  loading. Above a threshold loading, the average film thickness is virtually independent of the amount of excess bulk  $V_2O_5$  secondary phase ( $V_2O_5$  and anatase are essentially immiscible<sup>16</sup>). The SAF formation is presumably kinetically limited in the specimen containing  $\leq 2\%$   $V_2O_5$ . Third, even with the presence of excess ( $12\%$ – $30\%$ )  $V_2O_5$  secondary phase, the average film thickness does not increase with additional annealing time after an equilibrium state is reached [Fig. 2(b)]. Finally, Figs. 2(a) and 2(b) include specimens prepared by both dry and wet impregnation methods, which produce virtually the same results. The mean thickness ( $\pm 1$  standard deviation) for SAFs formed at  $600^\circ\text{C}$  in specimens prepared by the wet and dry impregnation methods is  $1.10\text{ nm}$  ( $\pm 0.28\text{ nm}$ ) and  $1.12\text{ nm}$  ( $\pm 0.22\text{ nm}$ ), respectively. Hence, it is concluded that these SAFs exhibit an equilibrium thickness.

In order to probe the thickness-temperature dependence and to identify any kinetic limitations to equilibration, the surficial films were allowed to approach their equilibrium state from both lower and higher temperatures. In the first instance, the samples were directly heated to a particular annealing temperature. In the second, the samples were first fired at a higher temperature of  $600^\circ\text{C}$ , at which thicker films are known to form, and then the temperature was lowered to the equilibration temperature. Fig. 3 shows the reversible temperature dependence to the film thickness. Film thickness decreases monotonically with decreasing temperature. Nanoscale SAFs vanish at  $\sim 450^\circ\text{C}$ , but monolayer/submonolayer adsorption should persist at lower temperatures. A hysteresis loop was also observed (Fig. 3).

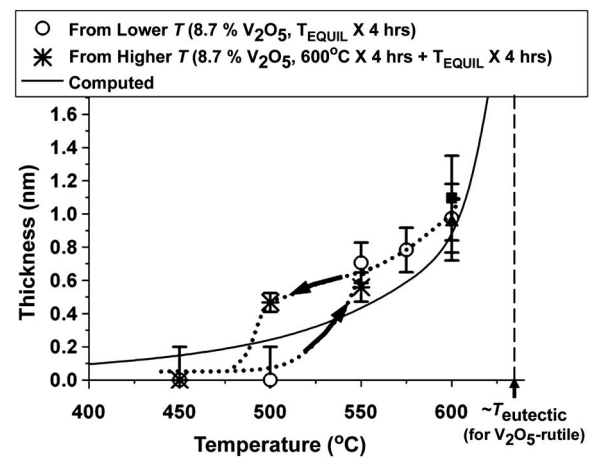


FIG. 3. Average film thickness vs equilibration temperature for two sets of specimens where the equilibrium states were approached from lower and higher temperatures, respectively. The overall average thickness for 119 SAFs formed at  $600^\circ\text{C}$  via different processing routes (■) and the mean thickness of SAFs formed in a specimen prepared with the MTI 99.99% anatase powder (Ref. 15) (▲) are also shown for comparison. The solid line was computed using Eq. (3) with the following parameters:  $\Delta T = (T - 631^\circ\text{C})$ ,  $\Delta S_f = 1.26\text{ mJ m}^{-2}\text{ nm}^{-1}\text{ K}^{-1}$ ,  $\xi = \sigma = 0.4\text{ nm}$ ,  $A_{123} = +263\text{ zJ}$ , and  $-\Delta\gamma_s \approx -\Delta\gamma + (A_{123}/12\pi\sigma^2) = 0.19\text{ J/m}^2$ . The dotted (trend) lines are added as a guide for the eyes.

The  $V_2O_5$  melting temperature is  $690^\circ\text{C}$  and the rutile- $V_2O_5$  eutectic temperature is  $\sim 631^\circ\text{C}$ .<sup>16</sup> These SAFs on anatase likely formed at subeutectic/subsolidus conditions (Fig. 3). Nonetheless, these subeutectic films are largely disordered (quasiliquid) in HRTEM [Figs. 1(a) and 1(b)]. Formation of crystalline surficial films is presumably frustrated by the high crystal-to-crystal interfacial energy that would occur. Analogous to the interfacial premelting theory,<sup>17</sup> the stabilization of a subeutectic, quasiliquid film can be conceived as if the increased free energy for forming the undercooled liquid film ( $\Delta G_{\text{amorph}}h$ ) is overcompensated by the reduction in interfacial energies ( $-\Delta\gamma$ ),

$$\begin{aligned} \Delta G_{\text{amorph}}h &= \Delta S_f \Delta T h < -\Delta\gamma \\ &\equiv -(\gamma_{V_2O_5} + \gamma_{\text{TiO}_2-V_2O_5} - \gamma_{\text{TiO}_2}^{(0)}), \end{aligned} \quad (1)$$

where  $h$  is the film thickness,  $\Delta S_f$  is the fusion entropy, and  $\gamma$ 's are the interfacial energies.<sup>2</sup> Stabilization of a  $1\text{ nm}$  thick subeutectic liquid film is thermodynamically favored for an undercooling ( $\Delta T$ ) range of

$$\begin{aligned} \Delta T &\equiv (T_{\text{eutectic}} - T) \leq \frac{-\Delta\gamma}{h\Delta S_f} \\ &\approx \frac{0.15\text{ J/m}^2}{(1\text{ nm})(0.00126\text{ J m}^{-2}\text{ nm}^{-1}\text{ K}^{-1})} \approx 120\text{ K}. \end{aligned} \quad (2)$$

The above rough estimation agrees well with the experimental observation (Fig. 3). Since  $0 < -\Delta\gamma < (\gamma_{\text{TiO}_2} - \gamma_{V_2O_5}) \approx 0.3\text{ J/m}^2$ , we adopted  $\Delta\gamma \approx 0.15\text{ J/m}^2$  in Eq. (2).  $\Delta S_f$  for  $V_2O_5$  was calculated from data in Ref. 18.

A more critical assessment of the equilibrium thickness should also consider the long-range dispersion force. The Hamaker constant was calculated to be  $+263\text{ zJ}$  for  $V_2O_5$  on anatase using a single oscillator approximation.<sup>19</sup> The corresponding pressure is attractive and  $\sim 14\text{ MPa}$  for a  $1\text{ nm}$

thick film. Consequently, the excess film free energy (referred to  $\gamma_{\text{TiO}_2}^{(0)}$  without any adsorption<sup>2</sup>) can be expressed in a simplified model,<sup>2,7</sup>

$$\Delta\sigma(h) = \Delta\gamma + \Delta S_f \Delta T h + \frac{-A_{123}}{12\pi(h^2 + \sigma^2)} + (-\Delta\gamma_s)e^{-h/\xi}, \quad (3)$$

which includes three  $h$ -dependent interactions: the amorphization energy, the dispersion interaction, and a short-range interaction. A SAF is stable if  $\Delta\sigma(h) < 0$ , and the equilibrium thickness corresponds to a local or global minimum in film energy versus thickness. Using Eq. (3), equilibrium thickness versus temperature was calculated and shown in Fig. 3. A refined model that considers mixing, through-thickness gradients, and electrostatic interactions is needed to yield more quantitative predictions. Nonetheless, agreement between the model predictions and experiments are satisfactory (Fig. 3). This proposed model is analogous to the phenomenological theories of premelting<sup>17</sup> and prewetting;<sup>20</sup> in-depth discussions of the thermodynamic models can be found in Ref. 2.

Although these SAFs appear to be largely disordered in HRTEM (Fig. 1), the existence of partial order has been predicated by the diffuse-interface<sup>7,21</sup> and atomistic<sup>22</sup> models. To reveal the existence of partial order, digital gray-level intensities of the HRTEM image were averaged along the horizontal axis [parallel to the (101) planes] in Fig. 1(c); partial layering order in this SAF was observed. The distance between the first two darkness peaks in the SAF was measured to be 0.43 nm, which matches the interlayer distance of the layered  $\text{V}_2\text{O}_5$  structure [Fig. 1(c)]. Since some order may have formed during the quench, a more critical assessment is not warranted.

Sanati *et al.* reported the formation of amorphous vanadia films at a lower temperature using  $\text{TiO}_2$  powders of lower purity (99%),<sup>12</sup> and the stabilization of SAFs at lower temperatures may be due to an impurity effect,<sup>9</sup> particularly in presence of “interacting” impurities.<sup>23</sup> This study demonstrated that these SAFs exhibit an equilibrium (instead of supply controlled) thickness that is tunable by varying equilibration temperature, akin to those observed for  $\text{Bi}_2\text{O}_3$  on  $\text{ZnO}$ .<sup>2,5-7</sup>

In summary, vanadia-based, equilibrium-thickness SAFs were observed to form on the (101) facets of  $\text{TiO}_2$  anatase particles. These quasiliquid films are stabilized in the subeutectic regime, where analogies to premelting and prewetting phenomena can be made. A reversible temperature dependence to film thickness was evident and explained. This

study collected a set of systematic data that are important for developing/validating generic thermodynamic models for equilibrium-thickness intergranular and surficial films. The existence of nanoscale SAFs of self-selecting thickness enables a route to tailor supported oxide catalysts, although a further study is needed to understand their catalytic properties.

Financial support from an NSF CAREER award (DMR-0448879) is acknowledged.

- <sup>1</sup>D. R. Clarke, *J. Am. Ceram. Soc.* **70**, 15 (1987); R. M. Cannon and L. Esposito, *Z. Metallkd.* **90**, 1002 (1999).
- <sup>2</sup>J. Luo, *Crit. Rev. Solid State Mater. Sci.* **32**, 67 (2007).
- <sup>3</sup>J. Luo, V. K. Gupta, D. H. Yoon, and H. M. Meyer, *Appl. Phys. Lett.* **87**, 231902 (2005); V. K. Gupta, D. H. Yoon, H. M. Meyer III, and J. Luo, *Acta Mater.* **55**, 3131 (2007).
- <sup>4</sup>A. Avishai, C. Scheu, and W. D. Kaplan, *Acta Mater.* **53**, 1559 (2005); C. Scheu, G. Dehm, and W. D. Kaplan, *J. Am. Ceram. Soc.* **84**, 623 (2000); M. Baram and W. D. Kaplan, *J. Mater. Sci.* **41**, 7775 (2006).
- <sup>5</sup>J. Luo and Y.-M. Chiang, *J. Eur. Ceram. Soc.* **19**, 697 (1999); *Acta Mater.* **48**, 4501 (2000).
- <sup>6</sup>J. Luo, Y.-M. Chiang, and R. M. Cannon, *Langmuir* **21**, 7358 (2005).
- <sup>7</sup>J. Luo, M. Tang, R. M. Cannon, W. C. Carter, and Y.-M. Chiang, *Mater. Sci. Eng., A* **422**, 19 (2006).
- <sup>8</sup>I. E. Wachs, L. E. Briand, J. M. Jehng, L. Burcham, and X. T. Gao, *Catal. Today* **57**, 323 (2000); B. M. Weckhuysen and D. E. Keller, *ibid.* **78**, 25 (2003).
- <sup>9</sup>I. E. Wachs and B. M. Weckhuysen, *Appl. Catal., A* **157**, 67 (1997).
- <sup>10</sup>Y.-C. Xie and Y.-Q. Tang, *Adv. Catal.* **31**, 1 (1990).
- <sup>11</sup>G. Centi, *Appl. Catal., A* **147**, 267 (1996).
- <sup>12</sup>M. Sanati, R. L. Wallenberg, A. Andersson, S. Jansen, and Y. Tu, *J. Catal.* **132**, 128 (1991).
- <sup>13</sup>X. T. Gao and I. E. Wachs, *Top. Catal.* **18**, 243 (2002).
- <sup>14</sup>A. Baiker, P. Dollenmeier, M. Glinski, and A. Reller, *Appl. Catal.* **35**, 351 (1987); Z. C. Kang and Q. X. Bao, *ibid.* **26**, 251 (1986).
- <sup>15</sup>Most specimens were prepared from anatase powder purchased from Sigma-Aldrich (5–15 nm nominal particle size; metallic impurities: 363 ppm K, 349 ppm Nb, 227 ppm Zr, and 39 ppm Ca; others <10 ppm). Purer (99.99%, 5–10 nm) anatase powder purchased from MTI Corp. was used for one case, which produced a virtually identical result (Fig. 3).
- <sup>16</sup>D. Habel, J. B. Stelzer, E. Feike, C. Schroder, A. Hosch, C. Hess, A. Knop-Gericke, J. Caro, and H. Schubert, *J. Eur. Ceram. Soc.* **26**, 3287 (2006).
- <sup>17</sup>J. G. Dash, *Contemp. Phys.* **30**, 89 (1989); J. G. Dash, A. M. Rempel, and J. S. Wettlaufer, *Rev. Mod. Phys.* **78**, 695 (2006).
- <sup>18</sup>G. V. Samsonov, *The Oxide Handbook*, 2nd ed. (Plenum, New York, 1982), pp. 34, 107, and 116.
- <sup>19</sup>R. H. French, *J. Am. Ceram. Soc.* **83**, 2117 (2000).
- <sup>20</sup>J. W. Cahn, *J. Chem. Phys.* **66**, 3667 (1977).
- <sup>21</sup>C. M. Bishop, R. M. Cannon, and W. C. Carter, *Acta Mater.* **53**, 4755 (2005); M. Tang, W. C. Carter, and R. M. Cannon, *Phys. Rev. Lett.* **97**, 075502 (2006).
- <sup>22</sup>S. Garofalini and W. Luo, *J. Am. Ceram. Soc.* **86**, 1741 (2003); W. D. Kaplan and Y. Kauffmann, *Annu. Rev. Mater. Res.* **36**, 1 (2006).
- <sup>23</sup>G. Deo and I. E. Wachs, *J. Catal.* **146**, 335 (1994).